HETEROCYCLES, Vol. 71, No. 12, 2007, pp. 2639 - 2658. © The Japan Institute of Heterocyclic Chemistry
Received, 17th June, 2007, Accepted, 30th August, 2007, Published online, 31st August, 2007. COM-07-11143

QUANTUM-CHEMICAL STUDY OF 1,2-BIS(DIMETHYLETHYLENEGUANIDINO)BENZENES

Davor Margetić,*[1] Waka Nakanishi,[2] Takuya Kumamoto,[2] and Tsutomu Ishikawa*[2]

[1]Laboratory for Physical-Organic Chemistry, Division of Organic Chemistry and Biochemistry, Ruđer Bošković Institute, Bijenička c. 54, 10001 Zagreb, Croatia, e-mail: margetid@emma.irb.hr

[2]Graduate School of Pharmaceutical Sciences, Chiba University, 1-33 Yayoi, Inage, Chiba 263-8522, Japan

Abstract – A series of 1,2-bis(dimethylethyleneguanidino)benzenes, (*o*-bisguanidinobenzenes) was investigated computationally using quantum-chemical calculations. The basicity of *o*-bisguanidinobenzenes was evaluated and compared with known molecules, to be comparable to these of neutral superbases such as 1,8-bis(dimethylethyleneguanidino)naphthalene and 1,8-bis(dimethylamino)naphthalene. Investigation of the influence of substituents on the rotational energies of *o*-bisguanidinobenzenes revealed that employed quantum-chemical calculations showed limited success in estimation of relative order of rotational barriers. Geometries of calculated metal complexes are in good accordance with experimental results. The most basic bidentate compounds form the most stable complexes, correlating basicity and complex stability.

INTRODUCTION

Guanidines are strong organic bases[1] which are extensively used for catalysis of different organic reactions.[2] Natural occurring products with guanidine moiety in their structure (such as tetrodotoxin and saxitoxin) possess strong biological activity.[3] Chemical modification of guanidines lead to their use as chiral auxiliaries in asymmetric synthesis (such as Michael reaction, TMS cyanation, azidation, silylation and epoxidation).[4] Experimental studies have shown that the incorporation of two guanidine fragments into single molecule could further increase their basicity, acting in a similar manner as proton sponges.[5,6] Furthermore, the correct geometrical orientations of two guanidine fragments could make these molecules to act as powerful bidentate ligands.

In order to design novel 1,2-bis(dimethylethyleneguanidino)benzenes, with enhanced basicity and chemical properties, a series of *o*-bisguanidinobenzenes and related guanidines depicted in Chart 1 were investigated computationally. These guanidines were compared to known organic superbases

1,8-bis(dimethylethyleneguanidino)naphthalene (DMEGN) (**8**), 1,8-bis(tetramethylguanidino)naphthalene (TMGN) (**9**) and 1,8-bis(dimethylamino)naphthalene (DMAN) (**10**). The aim of this quantum-chemical study was threefold: a) to evaluate the basicity of *o*-bisguanidinobenzenes and compare with known molecules, b) to investigate the influence of substituents on the rotational energies of *o*-bisguanidinobenzene[7], and c) to assess their metal complexation ability.

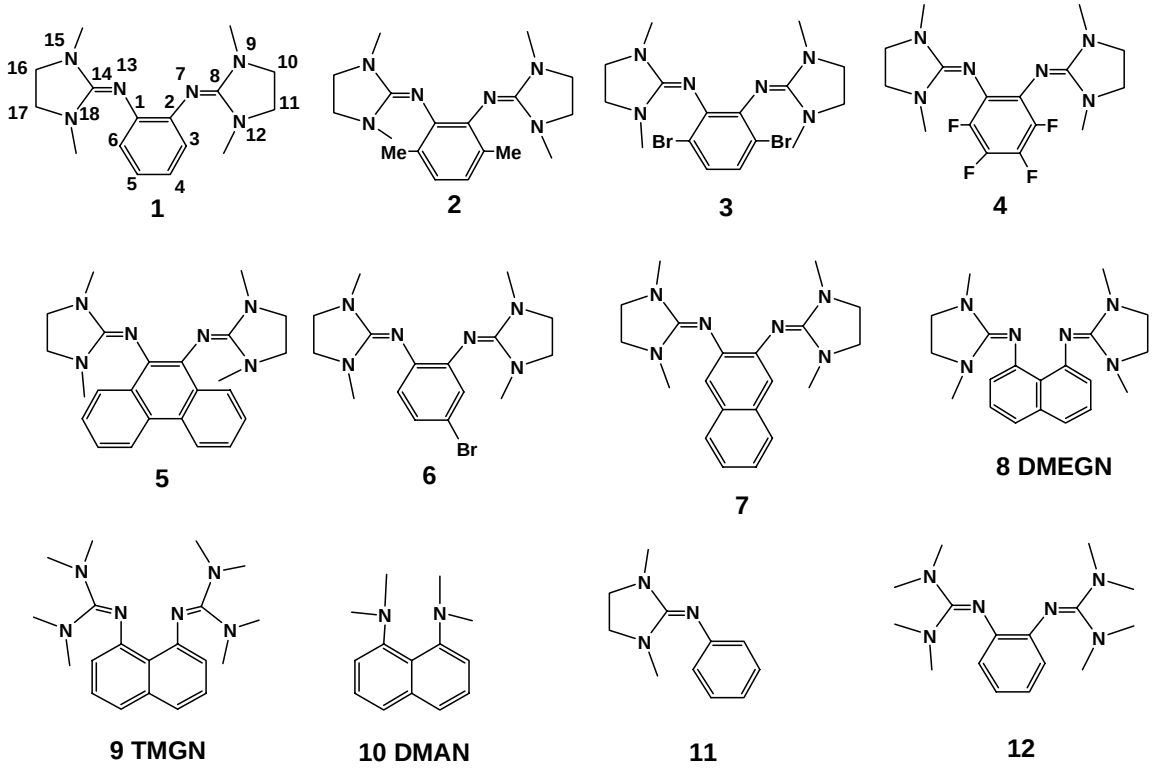

Chart 1 Calculated guanidines and numbering scheme used in this paper

RESULTS AND DISCUSSION

Computational results are collected in Tables 1-6 and depicted in Figures 1-5. Total molecular energies, zero-point vibrational energies (ZPVEs) and other data are listed in Supplementary material, which is available from authors, upon request.

MOLECULAR STRUCTURES OF *O*-BISGUANIDINOBENZENES AND THEIR PROTONATED FORMS

All guanidines have been optimized using RHF/6-31G* method and tables containing selected geometrical parameters are included in Supplementary material (S1). Two different conformations of *o*-bisguanidinobenzenes were located: as demonstrated for **1**, the first one (*cis*-**1**) has two dimethylethyleneguanidino rings oriented on the same side of benzene ring (Figure 1a), while the other conformation (*trans*-**1**) has guanidine rings on the opposite side, in respect to benzene plane (Figure 1b). RHF/6-31G* results show that *trans*-conformation (*trans*-**1**) is by 3.517 kcal mol^{-1} more stable than *cis*-**1** conformation ($\Delta E_{tot} = E_{tot}$(*cis*-**1**)-E_{tot}(*trans*-**1**) = 3.517 kcal mol^{-1}). Similar

energy difference between two conformers was found for their protonated forms *trans*-**1H** and *cis*-**1H** (2.93 kcal mol^{-1}) and also almost identical value was calculated[8] for diprotonated **TMGN** (**9H$_2$**) (3.5 kcal mol^{-1}). These results are in good accordance with published X-ray structures showing *trans*-orientation of two guanidine rings in several *o*-bisguanidinobenzene complexes. Furthermore, RHF/6-31G* calculated structural parameters (bond lengths, bond angles and dihedral angles) for *o*-bisguanidinobenzenes are in good accordance with available X-ray data (Figure 1 and S2). Structure of *trans*-**1H** was also calculated using larger basis set including diffuse and polarization functions at the RHF/6-311+G** level, but only minor geometrical differences were found as compared to the RHF/6-31G* structure.

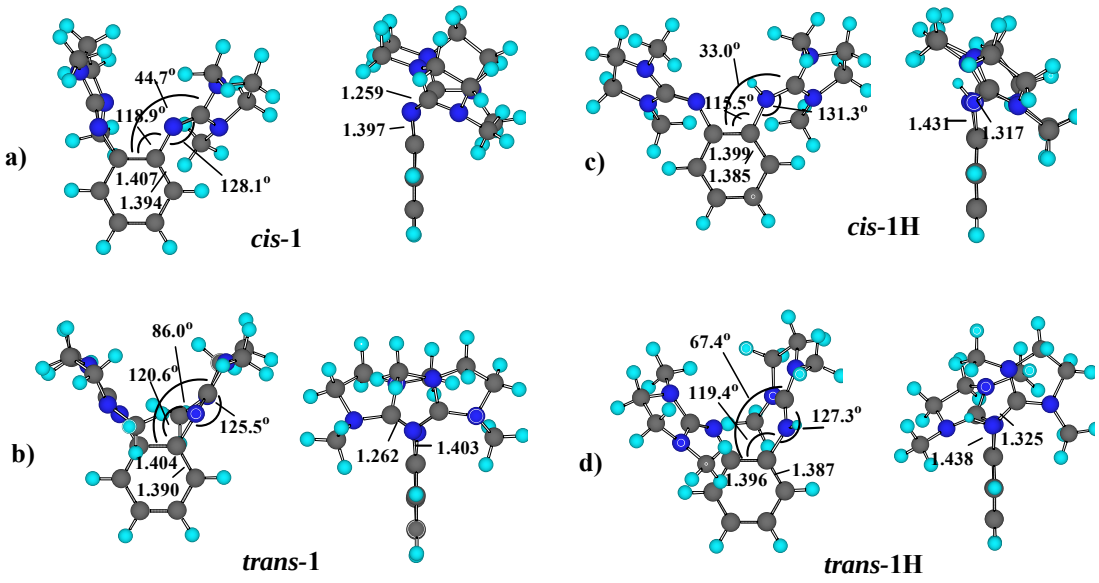

Figure 1 Optimized structures of a) ***cis*-1** and b) ***trans*-1** and their protonated forms c) ***cis*-1H** and d) ***trans*-1H**

A comparison of experimentally available X-ray results[9,10] and calculations of bisguanidines has revealed that RHF/6-31G* *ab initio* calculations are sufficient to predict geometrical parameters of studied molecules (Table 1, S3-S5). This statement holds for both neutral and protonated species. The largest differences between experiment and calculations could be found in the estimation of orientation of guanidine rings with respect to the aromatic ring (Θ), which was defined as an angle between $C_1C_2C_3$ and $C_2N_7C_8$ planes. For instance, calculated angle $\Theta(cis\text{-}\mathbf{1})_{HF}$ = 44.7°, while experimental angle $\Theta(cis\text{-}\mathbf{1})_{XR}$ = 54.7°. This difference may be the consequence of crystal packing forces, which are not included in the 6-31G* gas-phase calculations. However, it is important to note that all calculations correctly predict that *trans*-orientation of two guanidine rings is always energetically favored over *cis*-orientation. Furthermore, orientation of benzoic acid molecules complexing with bisguanidines as evidenced from crystal analysis was correctly modeled in the case of *trans*-**1** and phenanthrobisguanidine **5**. A comparison of results shows that benzoic acid orientation in respect to guanidine moiety in calculated and two available X-ray structures shows great degree of similarity. The most important conclusion from these calculations is that inclusion of complexation molecules (benzoic acid and benzyl alcohol) into calculations does not change significantly overall geometries of guanidines, as compared to calculation of isolated bis-guanidines.

Table 1 Comparison of experimental and calculation results for **1**, **3** and **5**

molecule	X-ray	average	calcs.	average
distance / Å				
C_1C_2	1.396-1.416	1.398	1.379-1.415	1.401
C_2N_7	1.392-1.435	1.409	1.397-1.418	1.402
$N_7{=}C_8$	1.251-1.309	1.289	1.259-1.286	1.276
C_8N_9	1.331-1.404	1.371	1.378-1.402	1.386
C_8N_{12}	1.322-1.453	1.363	1.374-1.393	1.383
N_9C_{10}	1.447-1.639	1.419	1.443-1.460	1.447
$C_{10}C_{11}$	1.468-1.526	1.436	1.493-1.521	1.512
$C_{11}N_{12}$	1.432-1.491	1.419	1.450-1.467	1.455
N_7N_{13}	2.699-2.886	2.801	2.798-2.854	2.813
angle / ^{o}				
$C_1C_2N_7$	117.2-121.3	118.7	118.9-120.9	120.1
$C_2N_7C_8$	121.7-126.3	124.0	122.5-128.1	125.7
$N_7C_8N_9$	109.9-130.5	121.2	120.1-122.4	120.7
$N_7C_8N_{12}$	120.9-132.6	126.1	129.3-132.6	131.5
$N_9C_8N_{12}$	108.0-112.6	109.3	107.3-108.2	107.6
dih. angle / ^{o}				
$C_8N_7C_2C_3$	24.2-76.7	47.8	52.6-92.9	76.4
$C_{14}N_{13}C_1C_6$	32.7-77.7	56.4	73.7-92.9	87.5
$C_8N_9C_{10}C_{11}$	6.3-29.7	20.5	27.3-31.1	28.6
$N_9C_{10}C_{11}N_{12}$	5.8-31.1	22.4	23.5-31.3	13.1

In all studied *o*-bisguanidinobenzenes protonation occurs on the one of guanidine imine nitrogens (N_7 or N_{13}), yielding unsymmetrical structures, as depicted for protonated forms of bases *cis*-**1** and *trans*-**1** in Figure 1. Similar unsymmetrical structures have been calculated for a series of diamines.[11] Geometrical changes induced by protonation are following: the C_2-N_7 and $N_7{=}C_8$ bonds are lengthened due to rehybridization by average 0.04 Å, while C_8-N_9 and C_8-N_{12} bonds are shortened (by ≈ 0.05 Å), due to increased resonance, accompanied by planarization of the protonated imino-nitrogen N_7 (ϕ= 17.7^o). The N_7-H_7 and N_{13}-H_7 distances in *cis*-**1H** and *trans*-**1H** (1.000, 2.268, 0.996 and 3.224 Å, respectively) differ significantly than those in **TMGNH** (0.910 and 1.750 Å) and **DMEGNH** (0.870 and 1.850 Å), showing intramolecular hydrogen bonding (IHB) between N_7 and N_{13} atoms. Finally, the N_7-N_{13} distance in *cis*-**1H** (2.785 Å) is larger than that in **TMGNH**, **DMEGNH** and **DMANH** (2.593, 2.590 and 2.717 Å, respectively).

The symmetrically protonated structures of *cis*-*(*and *trans*-*)***1H-TS** (where H^+ is bridging two imino nitrogens) has been also calculated and compared to the other bis-guanidines depicted in Chart 2. It was found that this species is transition state structure, possessing one imaginary frequency of vibration, $\nu^{\neq}$= 1930.4*i* cm^{-1}, which visualization shows that it corresponds to the motion of H^+ atom in $N_7 \leftrightarrow N_{13}$ direction. This structure has $N_7 \cdots H_7^+$ ($N_{13} \cdots H_7^+$) inter-atomic distances of equal length of 1.283 Å (Figure 2). Similar symmetrical structures were obtained for *cis*- and *trans*- **5H-TS**, **8H-TS** and **9H-TS**, possessing $N_7 \cdots H_7^+$ ($N_{13} \cdots H_7^+$) inter-atomic distance within 1.263 and 1.287 Å. Obtained TS structures experience smaller geometrical changes around imine nitrogen, as compared to non-symmetrically protonated *cis*-**1H** and *trans*-**1H**: elongation of $N_7{=}C_8$ bond by 0.050 Å (similar as in **1H**), however, in transition state structures there is almost no change in C_2-N_7 bond distance (by 0.010 Å, while in **1H** is much more pronounced, Δ= 0.035 Å). It was found that there is a largest N_7N_{13} distance contraction in **1H-TS**, as

compared to ground state geometries, indicating the extent of favorable intramolecular hydrogen bonding (IHB) interactions. The largest activation energy was predicted for **5H-TS** (27.19 kcal mol^{-1}), while the smallest for **8H-TS** (7.44 kcal mol^{-1}, Table 2). From these results it may be concluded that non-symmetrically protonated structures having proton located at one of two imine atoms are energetically favorable. These results are in good accordance with the structures of protonated bisguanidines obtained by X-ray crystallography.[12]

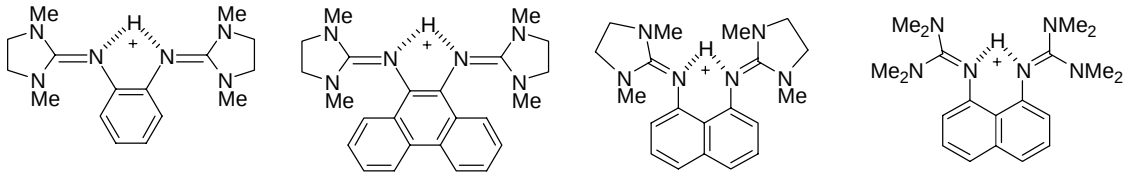

Chart 2 Symmetrically protonated guanidines

Table 2 RHF/6-31G* total energies for monoprotonated symmetrical forms (in a.u.), activation energies, imaginary frequencies of vibration and geometrical parameters

TS	E_{tot} (TS/start)	E_{act} (kcal/kJ mol^{-1})	$\nu^{\neq}$ (cm^{-1})	$N_7 \cdots H_7^+$ distance (Å)	N_7N_{13} distance (Å)	N_7N_{13} diff. (Å)
1H-TS	-946.93411	18.96 / 79.34	-1930.4	1.286	2.348	0.453
	-946.96433				(2.801)[a]	
5H-TS	-1252.23041	27.19 / 113.79	-1987.0	1.287	2.372	0.386
	-1252.27375				(2.758)	
8H-TS	-1099.59632	7.44 / 31.13	-1772.5	1.263	2.450	0.357
	-1099.60818				(2.813)	
9H-TS	-1101.88496	10.11 / 42.32	-1784.9	1.265	2.449	0.348
	-1101.90108				(2.797)	

[a] values for neutral bis-guanidines

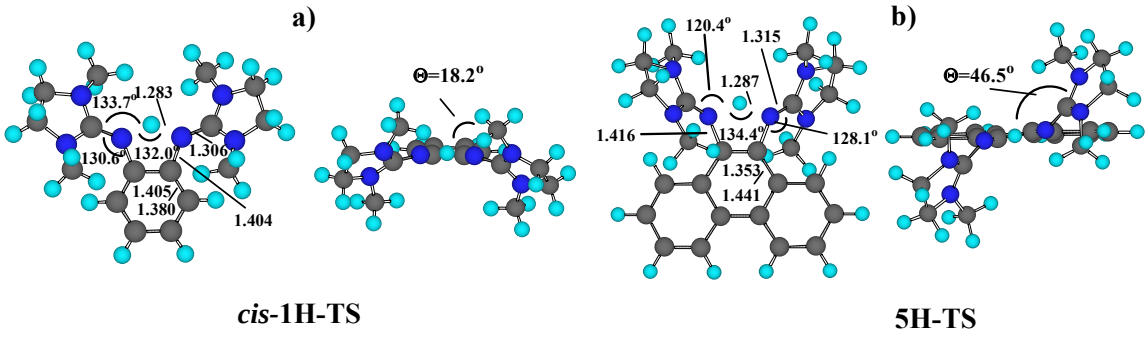

Figure 2 Optimized structures of symmetrically protonated guanidines ***cis*-1H** and **5H**

BASICITY OF *O*-BISGUANIDINOBENZENES

Absolute proton affinity (APA) of *o*-bisguanidinobenzene **1**[9] and related guanidines in the gas phase was calculated as described in Computational details section and results were collected in Table 3. These values are an important indicator of the activity of guanidines for their use as base catalysts for organic reactions.

Table 3 Absolute MP2 (APA_{MP2}) and HF_{SC} (APA_{HF}) proton affinities and pK_a(MeCN) values[a]

molecule	APA_{MP2} [b]	APA_{HF} [b]	pK_a(MeCN)
cis-**1**	246.7	250.2	20.5
trans-**1**	250.3	252.7	20.7
2	248.2	252.2	19.5
3	243.1	246.5	18.3
4	240.3	243.6	18.0
5	250.2	247.8	19.1
6	246.9	248.7	20.2
7	249.7	251.5	20.4
8[6]	250.8(2)	252.3(2)	23.0 (22.4)
9[16]	257.5	261.1	25.1
10[17]	245.5	240.7	18.2
11	239.6	242.8	17.2

[a] *trans*-orientation of two guanidine rings, [b] in kcal mol^{-1}

Calculations using different computational models indicate that *trans*-**1** is more basic than its *cis*-conformer *cis*-**1** by 3.6 kcal mol^{-1} at MP2 level (Table 3, APA_{MP2}). This difference could be mainly the consequence of larger sterical interactions of *cis*-**1** in its protonated form. Related conformational effects on the PA values in Schiff's bases have been also reported in literature.[13] Further increase in APA is mainly due to IHB, as a result of an interplay of IHB and decrease in the conjugative interaction with aromatic backbone. In order to estimate the existence and energy contribution of the IHB in **1**, homodesmotic reactions (1) and (2) have been considered.

$$\mathbf{1H} + \mathbf{benzene} \longrightarrow 2\times\mathbf{11} + \varepsilon_1 \qquad (1)$$

$$\mathbf{1H} + \mathbf{benzene} \longrightarrow \mathbf{11} + \mathbf{11H}^{+} + \varepsilon_1^{+} \qquad (2)$$

A small negative value of ε_1 indicates that unfavorable steric interactions and a stabilization of system **1** occuring due to a conjugative interaction between substituents and naphthalene moiety almost cancel out (*trans*-**1**, *cis*-**1** 0.99 and 4.51 kcal mol^{-1}, respectively, as obtained at RHF/6-31G* level, with ZPE corrections). A low negative ε_1^{+} values show that stabilization in *trans*-**1H** and *cis*-**1H** due to IHB are 9.81 and 6.88 kcal mol^{-1}, respectively. The effective IHB energies are similar as obtained previously for DMEGN and TMGN. Inability to form hydrogen bond between two nitrogen atoms causes that monoguanidine **11** has significantly smaller calculated APA value than *trans*-**1** (by 10.7 kcal mol^{-1} at MP2 level). Replacement of benzene with naphthalene ring in **7** slightly decreases APA as compared to *trans*-**1**. Substitution of aromatic ring in *trans*-**1** with electron withdrawing halogen atoms leads to decreased APAs in order tetrafluoro **4** < dibromo **3** < bromo **6** < *trans*-**1**. These estimations are in good accordance with literature data showing that aromatic substitution and electron withdrawing groups decrease APA of amines.[14,15] A comparison of proton affinities of *trans*-**1** with published value for bisguanidine **9**[16] (APA_{MP2} = 257.5 kcal mol^{-1}) reveals that **9** is much more basic than *trans*-**1**. Furthermore, a comparison with the APA of DMAN (**10**)[17] (APA_{MP2} = 245.5 kcal mol^{-1}) indicates that all of the studied *o*-bisguanidinobenzenes are of similar basicity or slightly more basic than DMAN due to the more effective reduction of lone pair repulsive interactions.

ROTATIONAL BARRIERS FOR *CIS/TRANS*-ISOMERISATION

In our search of *o*-bisguanidinobenzenes possessing potential chirality, based on restricted rotation of dimethylethyleneguanidino groups in respect to benzene moiety, rotational barriers of a series of molecules were estimated. *o*-Bisguanidinobenzenes possessing substituents at 3,6-positions of aromatic ring were chosen for the purpose of investigation of the influence of bulky substituents on rotational barrier. Also, for comparison, a related bis-guanidines **8** and **9** were modeled, while **12** was chosen to estimate the effects of acyclic guanidine. The following species were calculated: *trans*-**1**, **2**, **3**, **5**, **DMEGN** (**8**)**, TMGN** (**9**) and acyclic guanidine **12**. Also, their monoprotonated and bisprotonated forms were calculated: **1H**, **1H$_2$**, **2H**, **2H$_2$**, **3H**, **3H$_2$**, **5H**, **5H$_2$**, **DMEGNH**, **DMEGNH$_2$**, **TMGNH**, **TMGNH$_2$**, **12H** and **12H$_2$**.

Throughout the paper, rotations I and II are defined as rotations around single C_2-N_7 bond (I) and around imine N_7=C_8 bond (II). In the case of monoprotonated (or methylated) species, rotation refers to barrier involving the protonated (methylated) imine nitrogen N_7 moiety.

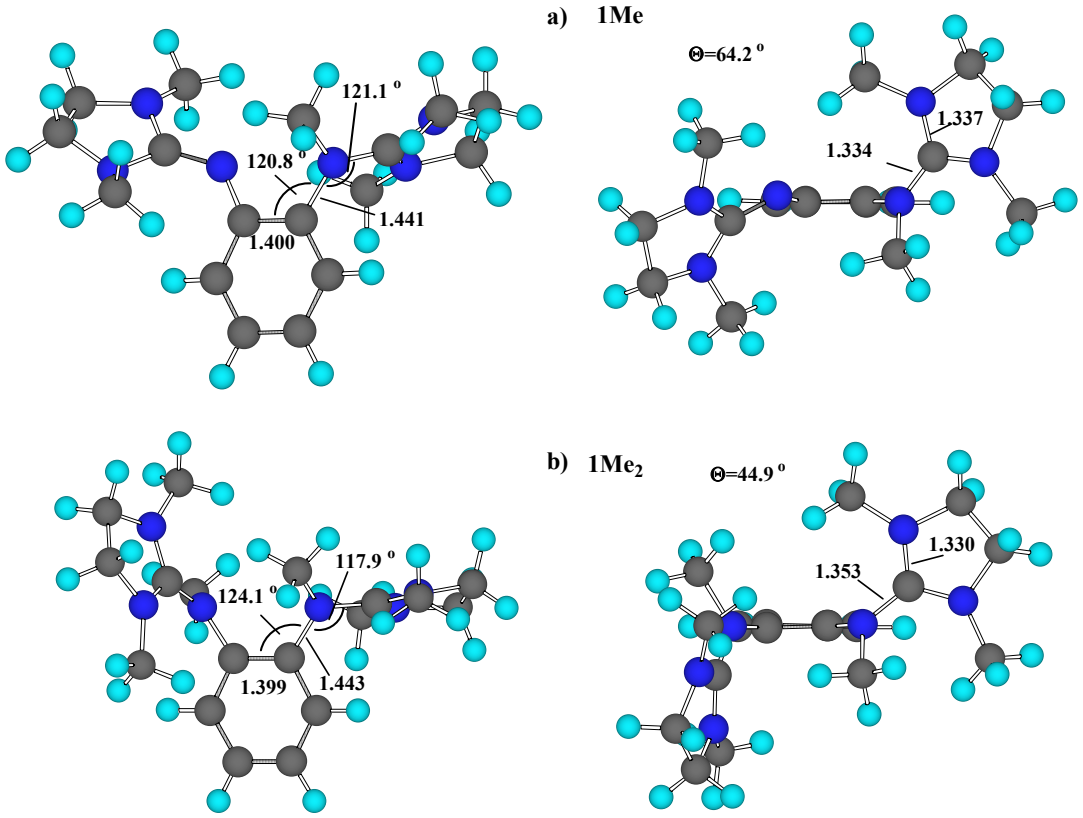

Figure 3. RHF/6-31G* optimized structures of **1Me** and **1Me$_2$**

COMPARISON OF METHYLATION WITH PROTONATION OF *O*-BISGUANIDINOBENZENES

Since bisprotonated and methylated *o*-bisguanidinobenzenes have not been discussed in previous sections, we shall start analysis with their comparison. While the attachment of second proton could occur at one of the amine

nitrogens within guanidine moiety, both theoretical and experimental[18] results show that the second proton attack occurs at the free imine nitrogen.[8] Similarly to neutral bases, our calculations indicate that bisprotonated (bismethylated) *trans*-conformations are thermodinamically more stable than *cis*-one. This could be attributed to the repulsion forces between two positively charged centers. The N_7-N_{13} distance in *trans*-**1** is larger (by 0.052 Å) than in *cis*-**1** resulting in weaker repulsion. Inspection of geometrical changes caused by (bis)methylation and bisprotonation of *o*- bisguanidinobenzenes (as calculated using RHF/6-31G* method) has revealed almost identical geometrical features, as earlier discussed for mono-protonation (Figure 3, S5). The most pronounced changes are the elongation of N_7=C_8 bond and shortening of C_8-N_9 and C_8-N_{12} bonds, as a consequence of cation delocalization within guanidine fragment. Furthermore, due to increased sterical demands, the N_7-N_{13} interatomic distance in *trans*-**1Me$_2$** is larger by 0.112 Å, as compared to neutral base *trans*-**1**. In such a sterically crowded situation, dimethylethyleneguanidino rings are further rotated in respect to benzene ring in **1Me** and **1Me$_2$** (by 64.2 and 44.9 ^{o}, respectively).

STEREODYNAMICS

Initial semiempirical PM5 calculations have led to the limited success in prediction of relative rotational barriers about C_2-N_7 bond for **1**, **5**, **12** and their protonated forms.[7] Both PM5 and experimental results agree that the barrier heights decrease in order **1** > **1H$_2$** > **1HMe**. On the other hand, experimental and PM5 computational results for **5** and **12** are contradictory. In the light of these results, more accurate quantum-chemical calculations were employed and results collected in Table 4. Due to the computational limits, instead of full geometry optimization using *ab initio* calculations, less computationally demanding single point DFT//semiempirical approach[19] was employed. In particular, full rotational barrier scan was performed using semiempirical AM1 method, followed by the estimation of single point energies at the B3LYP/6-31G* level (B3LYP/6-31G*//AM1). AM1 method was chosen, knowing that this approach have been shown to be in generally good agreement with the *ab initio* results for nitrogen containing molecules.[20] However, results obtained by AM1 method give similar predictions as PM5 calculations and will not be further discussed.

Conclusions which could be drawn from B3LYP/6-31G*//AM1 rotational barrier calculations (Table 4) are the following: Generally, rotation around N_7=C_8 bond has larger rotational barrier than rotation around C_2-N_7 bond. This finding is in accord with previously published calculations on related molecular systems.[20,21,22]

a) **Rotation around C_2-N_7 bond:** 1) bisguanidine **5** has the highest rotational barrier (E_{rot}), among *o*-bisguanidinobenzenes, while **1** has the smaller, substitution of **1** at positions 3- and 6- increases barrier, 2) naphthalene based bisguanidines **8** and **9** have higher E_{rot} than **1**; 3) protonation and bisprotonation decreases E_{rot}, while methylation increases: 4) acyclic bisguanidine **12** has the largest E_{rot} of all calculated species.

Table 4 Rotational barriers (E_{rot})[a]

Rotation	I C_2-N_7			II N_7=C_8		
	B3LYP	AM1	IPCM	B3LYP	AM1	IPCM
Guanidine						
1	2.0	5.1	3.0	9.3	16.1	3.3
2	4.8	15.2	3.8	12.0	16.5	4.5
3	4.6	-	3.5	4.5	-	4.9
5	5.3	19.3	5.8	6.4	21.1	6.9
1H	0.9	5.1	1.2	14.6	8.0	3.3
2H	2.5	12.0	0.5	21.9	10.8	1.8
3H	1.4	-	2.5	6.6	-	2.0
5H	4.0	14.4	3.6	10.8	16.1	5.7
$1H_2$	0.6	4.9	1.1	9.8	5.9	2.1
$2H_2$	1.1	6.0	0.7	18.7	9.4	1.4
$3H_2$	1.2	-	1.2	2.5	-	4.9
$5H_2$	2.7	7.9	1.4	9.2	8.2	1.6
8	8.0	10.3	4.2	17.1	18.5	5.1
9	8.9	7.7	3.1	18.1	9.1	3.1
8H	6.1	8.4	2.0	18.8	13.0	2.7
9H	7.5	5.6	2.7	23.4	7.2	2.8
1Me	9.6	8.7	3.2	12.3	12.3	4.7
$8H_2$	3.1	2.4	1.2	20.3	10.3	3.0
$9H_2$	4.8	3.9	2.6	24.4	7.5	2.7
$1Me_2$	7.6	5.8	2.4	13.5	7.6	3.9
1HMe-h[b]	8.9	4.5	1.8	14.5	5.6	2.2
1HMe-m[b]	9.5	4.3	1.3	15.1	4.7	2.3
12	11.5	4.6	6.0	14.6	4.4	7.0
12H	9.7	4.2	9.6	14.4	4.3	17.1
$12H_2$	6.5	2.9	7.9	13.6	3.5	14.9
12HMe	13.3	3.4	13.4	15.9	4.6	13.3

[a]AM1=PCM-AM1//AM1; B3LYP=B3LYP/6-31G*//AM1; IPCM=IPCM-B3LYP/6-31G*//AM1; Energies are given in kcal mol^{-1}; [b]h=rotation on protonated guanidine, m= rotation of methylated guanidine

b) **Rotation around N_7=C_8 bond:** 1) relative order of E_{rot} has changed from C_2-N_7 rotation; 2) protonation increases, but bisprotonation decreases E_{rot}; 3) bismethylation decreases E_{rot}.

In order to further refine predictivity of B3LYP/6-31G*//AM1 calculations, E_{rot} for *cis/trans*-isomerisation of *o*-bisguanidinobenzenes were also calculated with solvent effects taken into account. Therefore, single point PCM-AM1//AM1 and IPCM-B3LYP/6-31G*//AM1 calculations in acetone (ε=20.7) on AM1 optimized structures were conducted (results are summarized in Table 4). Initial PCM-AM1//AM1 calculations have indicated that rotation around N_7=C_8 bond has in all cases higher barrier than corresponding C_2-N_7 bond rotation, while protonation decreases E_{rot}. Since there are no parameters for bromine atom implemented in PCM-AM1 computational method, and due to poor correlation with the B3LYP/6-31G*//AM1 results, much more sophisticated calculations were employed, at the IPCM-B3LYP/6-31G*//AM1 level in acetone. Conclusions which

could be drawn from IPCM-B3LYP/6-31G*//AM1 calculations of E_{rot} are similar to the B3LYP/6-31G*//AM1 calculations: a) **Rotation around C_2-N_7 bond**: 1) relative order of E_{rot} is **5** > **2** > **3** > **1**, while **8** and **9** have higher E_{rot}; 2) protonation, bisprotonation and bismethylation decreases, while methylation increases E_{rot}; 3) acyclic **12** has the largest E_{rot} of all neutral species. b) **rotation around N_7=C_8 bond**: 1) relative order of E_{rot} is **5** > **3** > **2** > **1**; 2) protonation and bisprotonation decrease E_{rot}, while monoprotonation-methylation, methylation and bismethylation increase.

To ascertain predictivity of various quantum-chemical calculations for search of *o*-bisguanidinobenzenes possessing potential chirality based on restricted rotation, a comparison of computational results with the available experimental data was made. Table 5 contains experimental and computational results for series of bisguanidines, arranged in a decreasing order based on experimentally determined E_{rot}, from **12** to **5**. Although there are no published experimental data for bisguanidinobenzenes **2** and **3**, their computational results are also included for the sake of comparison. Dynamic NMR results[7] have shown that rotational barrier for acyclic *o*-bisguanidinobenzene **12** is the highest (11.9 kcal mol^{-1}), while **1HMe** has the smallest (relative order for **$1H_2$** and **1HMe** was obtained indirectly from dynamic NMR studies, without the estimation of their E_{rot}). We shall start the analysis of results in Table 5 with the comparison of energy differences between ground state *cis*- and *trans*-forms of guanidines (ΔE_1), obtained at the RHF/6-31G* level and further refined by addition of zero point vibrational corrections (ΔE_2). Amongst calculated species, *trans*-form of acyclic **12** is predicted to be the most stable, followed by *ortho*-substituted species **2**, **5** and **3**, indicating their potential existence as thermodinamically stable chiral structures. However, due to the small differences in energies, the relative order of ΔE_1 (ΔE_2) does not correlate well for other structures. The examination of results contained in Table 5 also indicate that experimental stereodynamic results do not correlate to the relative stability of *cis*- and *trans*-forms.

A comparison of calculated rotational barriers E_{a1}-E_{a6} (extracted from Table 4) to experiment reveals that calculations at all levels employed (B3LYP/6-31G*//AM1, PCM-AM1 and IPCM-B3LYP/6-31G*//AM1) predict wrong relative ordering of E_a for the most of guanidines. For instance, **12** has experimentally higher E_a than **1** and **5**, but calculations predict opposite, with B3LYP/6-31G*//AM1 being the only method predicting this result correctly. Furthermore, absolute E_a values obtained by calculations differ from experimental ones. In general, calculations for rotation about C_2-N_7 bond underestimate, while calculations for rotation about N_7=C_8 bond overestimate experimental values.

With an assumption that the energy for rotation should become the highest for the rotation angle being around ϕ= 180° (*i.e.* transition state), constrained optimizations were conducted at RHF/6-31G* level. In these calculations, rotational angle $C_1C_2N_7C_8$ (ϕ) was kept fixed to 180°, while all other geometrical parameters were fully optimized. Rotational energies obtained in such a way (E_{a7}) show reasonably good accordance with the relative order of experimental E_a: **12** was predicted to have the highest, followed by **9**, **$5H_2$**, **$8H_2$** and **1**. The only notable discrepancy was found for **5** and **3**, possessing calculated E_a higher than **$5H_2$**.

Since two mechanisms can be considered for *cis*-/*trans*- isomerization of guanidine molecules (one is C-N (or C=N) bond rotation and another is nitrogen inversion, or an intermediate mechanism with a high rotational component)[23], two additional sets of E_a were estimated for nitrogen inversion process, E_{a8} and E_{a9}. In the case of E_{a8},

the 6-31G*//AM1 energies were estimated for AM1 optimized transition state structures possessing $C_2N_7C_8$ angle fixed to 180°. E_{a9} denotes inversion E_a, calculated for 6-31G* optimized transition state structures possessing $C_2N_7C_8$ angle fixed to 180°. Inspection of the results reveals that both E_{a8} and E_{a9} incorrectly predict the highest E_a for guanidines **8H₂** and **5H₂**. There is a large discrepancy to experiment for neutral, protonated and quaternized species, which presumably arises from the strain in TS geometries imposed by $C_2N_7H_7$ bond angle of almost 90°. In addition, for the selected *o*-bisguanidinobenzenes, single point estimation of E_a, using a larger basis set, including polarization and diffusion functions (B3LYP/6-311+G**//AM1 method) was employed. These calculations have shown a limited success in prediction of the relative E_a.

Table 5 Comparison of experimental and computational results for rotational barriers (in kcal mol^{-1})[a]

				C_2-N_7	C_2-N_7	C_2-N_7	N_7=C_8	N_7=C_8	N_7=C_8	N_7=C_8		
	expt	ΔE_1	ΔE_2	E_{a1}	E_{a2}	E_{a3}	E_{a4}	E_{a5}	E_{a6}	E_{a7}	E_{a8}	E_{a9}
12	11.9	10.9	10.7	11.5	4.6	6.0	14.6	4.4	7.0	19.4	43.8	19.9
9 [8]	11.8	2.9	2.6	8.9	7.7	3.1	18.1	9.1	3.1	11.8	40.5	20.5
5H₂	10.5	4.2	4.2	2.7	7.9	1.4	9.2	8.2	1.6	10.9	56.4	57.1
8H₂ [6]	9.1	3.9	3.7	3.1	2.4	1.2	20.3	10.3	3.0	8.8	63.9	47.9
1	8.6	3.5	3.6	2.0	5.1	3.0	14.1	16.1	3.3	7.7	17.9	16.9
5	8.5	4.8	4.8	5.3	19.3	5.8	6.4	21.1	6.9	15.5	27.0	12.8
1H₂		3.3	3.3	0.6	4.9	1.1	9.8	5.9	2.1	2.5	47.4	44.4
1HMe[b]		0.9	0.9	9.5	4.3	1.3	15.1	4.7	2.3	3.5	61.2	49.9
2 Me		6.1	6.1	4.8	15.2	3.8	12.0	16.5	4.5	9.1	15.3	16.9
3 Br		4.2	4.2	4.6	-	3.5	4.5	-	4.9	12.7	26.8	11.6

[a]ΔE_1=E_{tot}(*cis*-)-E_{tot}(*trans*-); ΔE_2=E_{tot}(*cis*-)-E_{tot}(*trans*-)+ZPE; E_{a1}=E_a(B3LYP/6-31G*//AM1); E_{a2}=E_a(PCM-AM1); E_{a3}=E_a(IPCM-B3LYP/6-31G*//AM1); E_{a4}=E_a(B3LYP/6-31G*//AM1); E_{a5}=E_a(PCM-AM1); E_{a6}=E_a(IPCM-B3LYP /6-31G*//AM1); E_{a7}=6-31G* constrained rotation ϕ=180°; E_{a8}=6-31G*//AM1 inversion, $C_2N_7C_8$ angle 180°; E_{a9}=6-31G* inversion, $C_2N_7C_8$ angle 180°; [b] computational results for rotation on methylated side (**1HMe-m**)

From the all above-mentioned results, it may be concluded that employed quantum-chemical calculations showed limited success in estimation of rotational barriers. These discrepancies may have arisen from the complexity of the interplay of several processes, involving C-N (or C=N) bond rotation, nitrogen inversion, quaternization, lone pair repulsion and overall electronic interactions.[24] The discrimination between nitrogen inversion and rotation mechanisms is difficult, indicating that the computational models with only one changeable parameter are unsuitable to correctly estimate stereodynamic processes in *o*-bisguanidinobenzenes.[25] Computation of stereodynamics of studied systems is further complicated by the possession of two guanidino moieties in close proximity imposing steric interactions, with a possibility of intramolecular hydrogen bonding and rapidly equilibrating proton between two guanidines.[12] Calculations previously published on this subject deal with simple model monoguanidines, in almost all cases without substituents, while the employed theoretical levels vary.[26] It is also important to point out that AM1 method used for the location of transition state structures in gas phase may not fully describe structures possessing non-bonding interactions such as IHB, which in turn leads to inconsistency in estimation of relative E_a. The other reasons for the discrepancy of computational and experimental results could

arise from the non-adequate modeling of intricate electronic processes such as hyperconjugative $n_{(Namine)} \rightarrow \pi^*_{(C\text{-}Nimine)}$ delocalization[27] or C=N bond conjugation with the adjacent aromatic system[28] in transition state. Although these calculations provide a good start to understanding conformational behavior of *o*-bisbenzoguanidines, it is clear that high-level calculations taking into account rotation and inversion simultaneously with IHB will ultimately be required. Keeping in mind all the pitfalls of calculations described above, several general points may be taken, which are particularly important for our search of suitable molecules possessing hindered rotation: substitution at 3,6-positions increases barrier (molecule **5**), acyclic guanidine **12** has larger rotational barrier than cyclic and quaternization in most cases lowers rotational barrier.

O-BIS-BENZOGUANIDINE-METAL COMPLEXES

In order to ascertain if there is a correlation between basicity and thermodynamic stability of guanidine-metal complexes, a series of bis-ligated metal complexes **1M**-**15M** (depicted in Chart 3, M = metal) was investigated by density functional quantum-chemical calculations employing B3LYP/LANL2DZ method. Their total energies are collected in Table S3. Selected average geometrical parameters of the calculated and experimentally determined structures of *o*-bisguanidinobenzene-metal complexes are shown in Table 6 (S6 (*cis*-**1**) and S7 (*trans*-**1**)). Also, optimized structures of several complexes are illustrated in Figures 4 and 5.

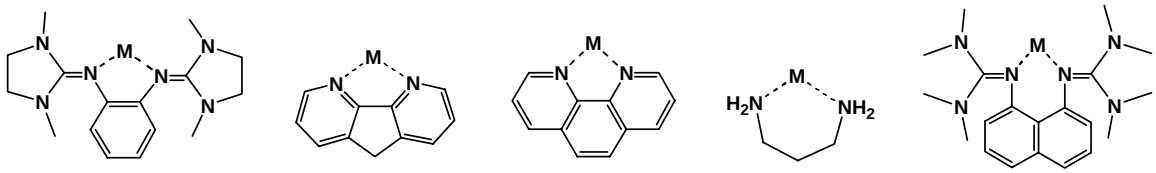

Chart 3 Bis-ligated metal complexes

Table 6 Comparison of experimental results and calculations for metal complexes

molecule	expt. [a,c]	**1M** calcs. [b,d]
distance / Å		
C_2N_7	1.429-1.483 [a]	1.417-1.423 [b]
$N_7{=}C_8$	1.262-1.340 [a]	1.338-1.356 [b]
C_8N_9	1.319-1.385 [c]	1.360-1.379 [d]
N_7N_{13}	2.507-2.992	2.564-2.806
N_7M_{19}	1.924-2.390	1.951-2.370
$M_{19}Cl_{20}$	2.226-2.397	2.304-2.409
angle / [o]		
$C_2N_7C_8$	115.3-126.8	122.9-124.3
$N_7C_8N_9$	114.9-123.9	122.1-128.8
$N_9C_8N_{12}$	113.6-120.2 [c]	108.9-110.0 [d]
$N_7M_{19}N_{13}$	72.7-113.1	79.7-83.2

[a] aliphatic substituents at N_7; [a] aromatic substituents at N_7; [c] alicyclic substituents at N_9; [d] cyclic substituents at N_9

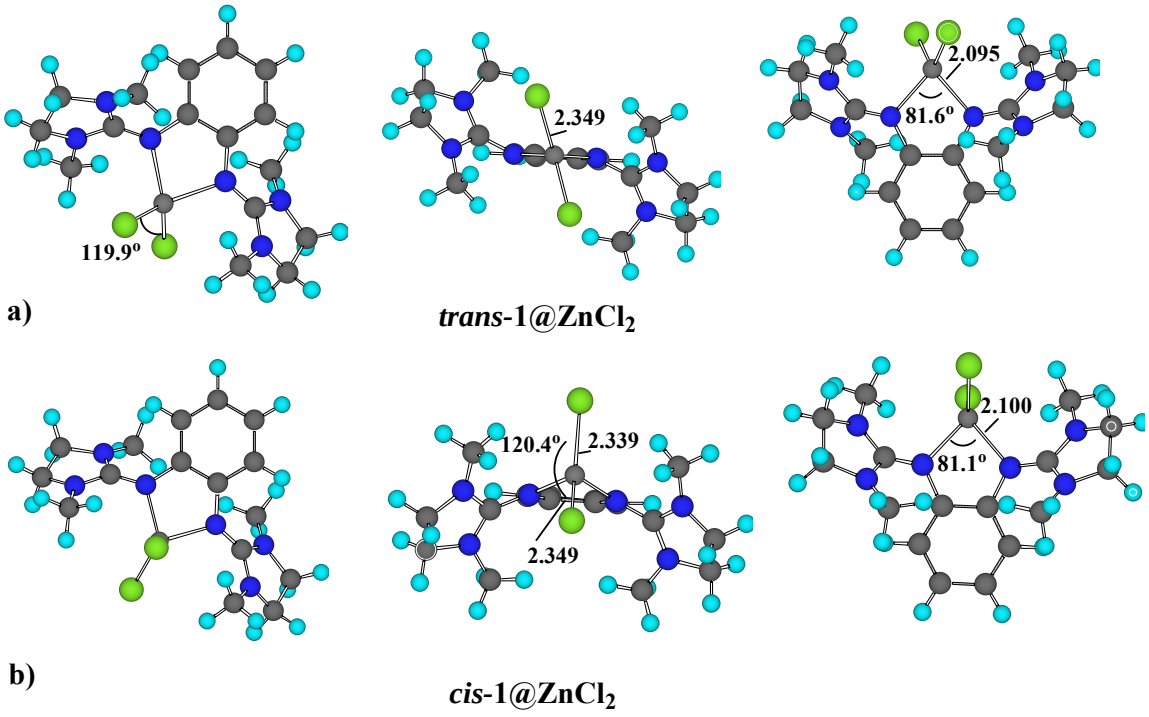

Figure 4 B3LYP/LANL2DZ optimized structures of *trans*- and *cis*-**1@ZnCl$_2$** complexes

MOLECULAR STRUCTURES OF O-BISGUANIDINOBENZENE-METAL COMPLEXES

Obtained density functional theory (DFT) structures (Figures 4 and 5) revealed that guanidines are encountered in coordination chemistry as neutral guanidine ligands with different metals, forming guanidine-metal complexes of MCl_2L_2 type. This finding is in accord to our observations that mixing of *o*-bisguanidinobenzene with metal salts affords solid complexes. These experimental results will be reported elsewhere.[10] The analysis of computational results has revealed that the MN and MCl distances of *o*-bisguanidinobenzene-metal complexes obtained by B3LYP/LANL2DZ calculations are in good agreement with the literature (Table 6). Other geometrical parameters are also close to the values of experimental structures. The differences which arise between experiment and DFT calculations are mainly the consequence of the studied guanidine systems (experimental structures possess aliphatic substituents at N_7 and alicyclic substituents at N_9, while computed structures have aromatic substituents at N_7 and cyclic substituents at N_9). However, experimental and calculated structures show the main common feature: in guanidine complexes, coordination occurs almost exclusively through the donation of the lone-pair electrons of the N^{imine} atom to the appropriate acceptor orbitals of the metal. Also the values of NMN and ClMCl angles are closely compared with that expected for a tetracoordinated complexes.[29] In metal complexes with *o*-bisguanidinobenzene ligand, slightly distorted tetrahedral coordination of metal atom was predicted, directed by steric restrictions for formation of square-planar geometry. For all metals studied, *trans*-form of complex is predicted to be thermodynamically favored. Complexes containing a bisguanidine ligand **1** possess the Cu and Pd atoms tetracoordinated in a planar quadratic manner by two guanidine N atoms and the two Cl atoms, while Fe atom is coordinated in a tetrahedral manner. These chelate heterocycles adopt a chair conformation.[30] Good structural agreement between calculated structures and related literature examples was also found for diazafluorene and phenanthroline complexes.[31,32] In ligands with diazafluorene **13**, phenanthroline **14** and DMAN (**10**), both distorted

tetrahedral (Cu, Fe and Zn atoms) and distorted square planar (Pd and Cu) geometries were obtained.

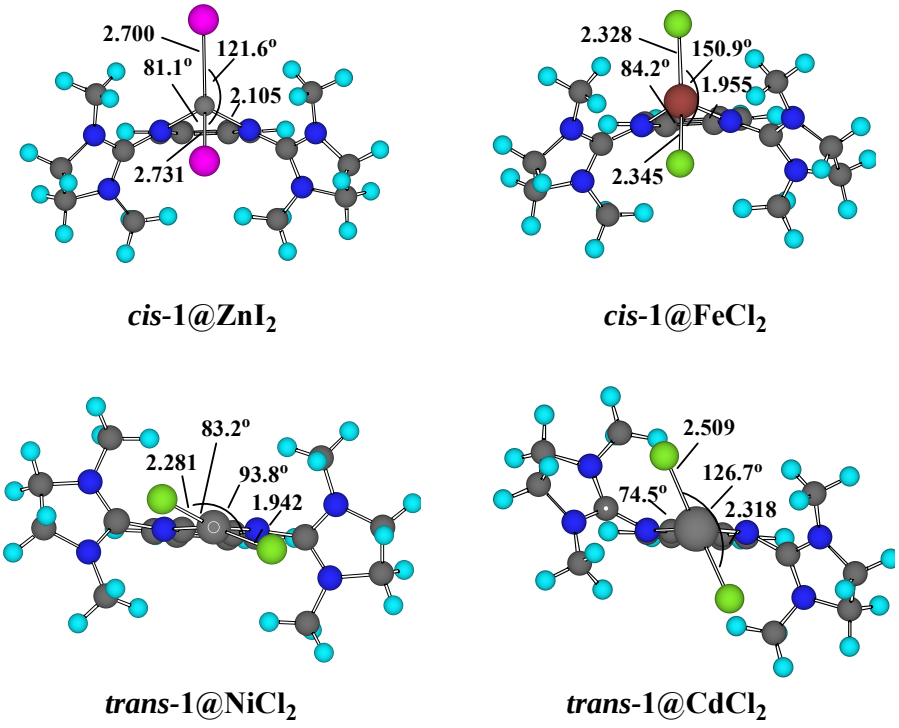

Figure 5 B3LYP/LANL2DZ optimized structures of *trans*- and *cis*-**1** complexes with metal chlorides

In continuation of study, absolute proton affinities (APA_{HF}) of bases depicted in Chart 3 in the gas phase were estimated using the computational procedure described in details above (Table 7). Their respective values of **1**, **13**, **14**, **15** and **10** are 250.2, 229.7, 210.2, 227.1 and 240.7 kcal mol^{-1}. On the basis of these values, relative basicity order based on calculated APA_{HF} is: **1** > **10** > **13** > **15** > **14**. Calculated APA_{MP2} and pK_a(MeCN) values indicate the same order (Table 1).

Table 7 Absolute MP2 and HF proton affinities and pK_a(MeCN) values

molecule	APA_{MP2} [a]	APA_{HF} [a]	pK_a(MeCN)
1	246.7	250.2	20.5
13	228.7	229.7	17.2
14	223.3	210.2	16.3
15	227.1	227.1	16.6
10 [8]	245.5	240.7	18.2

[a] in kcal mol^{-1}

Isodesmic reaction defined in Equation (3) (i.e. exchange of metals from one base to another) was used to estimate reaction energies and relative stability of complexes.

$$L_1M + L_2 \longrightarrow L_1 + L_2M \qquad (3)$$

Table 8 B3LYP/LANL2DZ energies of isodesmic reactions (defined in eq. 1)[a]

M	**1M+13→1+13M**	1M+14→1+14M	**1M+15→1+15M**	**1M+10→1+10M**
Li^+	77.7	75.9	30.1	27.5
Na^+	65.9	69.2	28.5	26.5
K^+	62.9	67.9	28.6	24.2
Cs^+	60.9	66.1	24.1	23.1
Ba^{+2}	84.9	89.2	59.1	50.4
Ca^{+2}	90.3	92.8	65.4	51.2
Sr^{+2}	90.7	94.3	65.4	55.4
$ZnCl_2$	82.6	78.3	26.2	22.0
$PdCl_2$	73.5	63.9	17.2	23.5
$FeCl_2$	78.5	66.6	16.5	14.9
$CuCl_2$	82.6	78.9	25.1	21.0

[a] kcal mol^{-1}

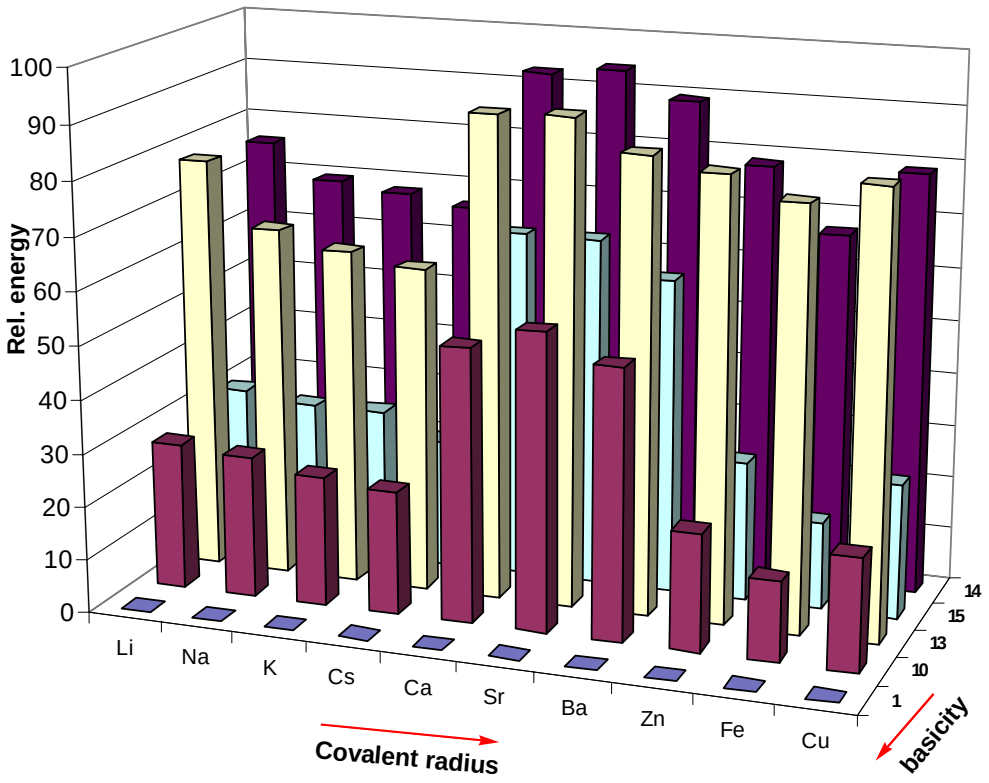

Figure 6 Comparison of calculated complexation energies of bis-ligands with basicity and the metal covalent radius (complexation energies of **1** are used as reference)

Results for these isodesmic reactions calculated for number of divalent metals and cations are collected in Table 8 (and reaction energies in S2). These calculations indicate the following order of complex stability: **1M** > **10M** , **15M** >> **13M** , **14M**. There is straightforward correlation found between basicity and complex stability for two most basic bidentate compounds, **1** and **10**, which have the most stable complexes, while smaller complex stability was calculated for less basic compounds **13** and **14** (Figure 6). High complex stability was found for propylene diamine **15**, which is opposite than predicted on the basis of its low basicity (APA_{HF}). This discrepancy may be

rationalized by the influence of bigger conformational flexibility of this bidentate ligand on complex stability, as compared to the other more rigid ligands studied here. Figure 6 also indicates that direct correlation of relative complexation energies and covalent radii is not established. While the relative energy decreases going from Li, Na, K to Cs, with the increase of covalent radius, there is sudden increase for Ca, Sr and Ba, then followed by smaller energies for Zn, Fe and Cu. No straightforward correlation was found between ionic radius and N-N ligand separation or N-Me bond lengths. Factors influencing σ-donating and π-accepting properties of the ligand N atom, the covalent radius, coordination modes and overall geometrical arrangement of bidentate ligands define their overall coordination properties.

Furthermore, complexation energies[33] for a series of *o*-bisguanidinobenzene reactions with metal dichlorides were also calculated and these results are summarized in Table 9 (S4). The inspection of these results reveals that complexation reaction of the platinum dichloride is the most exothermic, indicating that this complex is thermodynamically more stable than other complexes calculated in this study.[34] Based on these results, complex stability decreases in the following order:

$$PtCl_2 > FeCl_2 > PdCl_2 > CoCl_2 > ZnCl_2 > NiCl_2 \approx CuCl_2 > ZnI_2 > CdCl_2$$

The complexation energies of the metal complexes, calculated in this work follow almost the same order with some exceptions. The binding affinities have been found to be higher for Cu(II) and Ni(II) than for Co(II), violating the Irving-Williams order.[35] Such deviations are to be expected, since the Irving-Williams series of complex stabilities is valid for complexes in solution, while the present calculations refer to the gas phase. The binding affinity has been found to be maximum for Pt(II).

Table 9 B3LYP/LANL2DZ energies of complexation reactions[a]

	1+MCl_2→1MCl_2	**1+MCl_2→1MCl_2**
M	*cis*-	*trans*-
$CoCl_2$	-74.99	-73.56
$CdCl_2$	-54.28	-53.33
$NiCl_2$	-64.83	-63.06
$ZnCl_2$	-68.36	-67.02
ZnI_2	-60.98	-59.89
$CuCl_2$	-61.09	-63.11
$FeCl_2$	-97.82	-94.75
$PdCl_2$	-85.15	-80.05
$PtCl_2$	-102.3	-97.27

[a] kcal mol^{-1}

CONCLUSION

Ab initio RHF/6-31G* calculations correctly predict geometrical parameters of studied bisguanidines, as compared to experimentally available data. This statement holds for both neutral and protonated species. Basicity of *o*-bisguanidinobenzene is high and comparable to these of known superbases such as TMEGN and DMAN. Employed quantum-chemical calculations showed limited success in estimation of relative order of rotational barriers. Geometries of calculated metal complexes are in good accordance with experimental results. The most basic bidentate compounds form the most stable complexes, correlating basicity and complex stability.

ACKNOWLEDGEMENTS

Financial support of the Ministry of science, education and sport of Croatia, project No. 0098147 is gratefully acknowledged.

COMPUTATIONAL DETAILS

All calculations were carried out on Isabella computer cluster (24 dual processor HP ProLiant BLP20p nodes with Intel Xeon 2.8 GHz, 32 dual processor Dell 1850 1U nodes with Intel Xeon 3.4 GHz and 24 dual processor Pyramid GX28 nodes with AMD Opteron 248). Geometry optimizations were carried out with the *Gaussian 03* suite of programs[36] employing RHF/6-31G* and B3LYP/LANL2DZ methods. Harmonic vibration frequencies were calculated for all localized stationary structures to verify whether they are minima. Single point calculations were conducted using MP2(fc)/6-311+G**//RHF/6-31G* method, while solvation effects were calculated using IPCM/B3LYP/6-311+G**//RHF/6-31G* approach.[37-39] Semiempirical AM1 method was employed using Gaussian03 rotational search routine, in 90 steps using 2^o incremental steps. Solvation calculations were performed in the presence of a solvent polarizable continuum (PCM) model, developed by Mennucci and Tomasi.[40] Dielectric constant for acetone ε=20.7 was used. Absolute proton affinity of guanidines in the gas phase was calculated using the equations (4)-(6) described by Maksić and Kovačević[41]:

$$APA(B) = \Delta E_{el} + \Delta ZPVE \quad (4)$$

$$\Delta E_{el} = E(B)_{MP2} - E(BH^+)_{MP2} \quad (5)$$

$$\Delta ZPVE = ZPVE(B)_{HF} - ZPVE(BH^+)_{HF} \quad (6)$$

Here HF denotes RHF/6-31G* level; while MP2 is MP2(fc)/6-311+G**//RHF/6-31G* model. A somewhat less accurate but computationally more efficient model is the scaled Hartree-Fock (HF_{SC}) scheme based on the equation (7):

$$APA(B) = 0.8924\Delta E_{el(HF/6\text{-}31G^*)} + 10.4 \text{ kcal mol}^{-1} \quad (7)$$

Estimation of pK_a values in acetonitrile was achieved by using the equations (8)-(11):[41]

$$pK_a = 0.4953PA(B_{MeCN}) - 119.7 \quad (8)$$

$$PA(B_{MeCN}) = \Delta E_{el\ MeCN} + \Delta ZPVE_{HF} \quad (9)$$

$$\Delta E_{el\ MeCN} = E(B)_{MeCN} - E(BH^+)_{MeCN} \quad (10)$$

$$\Delta ZPVE_{HF} = ZPVE(B_{HF}) - ZPVE(BH^+_{HF}) \quad (11)$$

In these equations MeCN denotes IPCM/B3LYP/6-311+G**//RHF/6-31G* model and HF denotes RHF/6-31G* method).

REFERENCES AND NOTES

1. M. Costa, G. P. Chiusoli, D. Taffurelli, and G. Dalmonego, *J. Chem. Soc., Perkin. Trans. 1,* 1998, 1541.

2. Cyanation of aldehydes: S. Inoue, A. Mori, and K. Tanaka, *J. Org. Chem.,* 1990, **55**, 181; Strecker reaction: E. J. Corey and M. J. Grogan, *Org. Lett.,* 1999, **1**, 157; Transesterification: U. Schuchardt, R. Sercheli, and R. M. Vargas, *J. Braz. Chem. Soc.,* 1999, **9**, 199; Aldol condensation: A. Zhu, T. Jiang, D. Wang, B. Han, L. Liu, J. Huang, J. Zhang, and D. Sun, *Green Chem.,* 2005, **7**, 514: Michael reaction: Y. V. Subba Rao, D. E. De Vos, and P. A. Jacobs, *Angew. Chem., Int. Ed. Engl.,* 1997, **36**, 2661.
3. T. Nishikawa, D. Urabe, and M. Isobe, *Angew. Chem. Int. Ed.,* 2004, **43**, 4782; H. Tanino, T. Nakata, T. Kaneko, and Y. Kishi, *J. Am. Chem. Soc.,* 1977, **99**, 2818; K. Nagasawa, *Yakugaku Zasshi,* 2003, **123**, 387.
4. T. Ishikawa and T. Isobe, *Chem. Eur. J.,* 2002, **8**, 553; T. Kumamoto, K. Ebine, M. Endo, Y. Araki, Y. Fushimi, I. Miyamoto, T. Ishikawa, T. Isobe, and K. Fukuda, *Heterocycles,* 2005, **65**, 347.
5. R. W. Alder, P. S. Bowman, W. R. S. Steele, and D. R. Winterman, *Chem. Commun.,* 1968, 723.
6. V. Raab, K. Harms, J. Sundermeyer, B. Kovačević, and Z. B. Maksić, *J. Org. Chem.,* 2003, **68**, 8790.
7. Unpublished theoretical data. The experimental results: W. Nakanishi, T. Ishikawa, and D. Margetić, *Bull. Chem. Soc. Jpn.,* 2007, **80**, 1187.
8. B. Kovačević and Z. B. Maksić, *Chem. Eur. J.,* 2002, **8**, 1694.
9. M. Kawahata, K. Yamaguchi, and T. Ishikawa, *Cryst. Growth & Design,* 2005, **5**, 373.
10. W. Nakanishi, T. Ishikawa, (Chiba University); K. Kawahata, K. Yamaguchi, (Tokushima Bunri University), unpublished results.
11. S. Yamabe, K. Hirao, and H. Wasada, *J. Phys. Chem.,* 1992, **96**, 10261.
12. V. Raab, J. Kipke, R. M. Gschwind, and J. Sundermeyer, *Chem. Eur. J.,* 2002, **8**, 1682.
13. E. Tajkhorshid, B. Paisz, and S. Suhai, *J. Phys. Chem. B,* 1997, **101**, 8021.
14. F. D'Souza, M. E. Zandler, G. R. Deviprasad, and W. Kutner, *J. Phys. Chem. A,* 2000, **104**, 6887.
15. E. P. Hunter and S. G. Lias, 'Proton Affinity Evaluation' in NIST Chemistry WebBook, NIST Standard Reference Database Number 69, ed. by P. J. Linstrom and W. G. Mallard, March 2003, National Institute of Standards and Technology, Gaithersburg MD, 20899 (http://webbook.nist.gov).
16. B. Kovačević, Z. Glasovac, and Z. B. Maksić, *J. Phys. Org. Chem.,* 2002, **15**, 765.
17. H. Staab and T. Saupe, *Angew. Chem. Int. Ed.,* 1988, **27**, 865.
18. G. A. Olah, A. Burrichter, G. Rasul, M. Hachoumy, and G. K. S. Prakash, *J. Am. Chem. Soc.,* 1997, **119**, 12929.
19. B. S. Juršić, *Theochem,* 1998, **454**, 105; B. S. Juršić, *Theor. and Comp. Chem.,* 1996, **4** (Recent Developments and Applications of Modern Density Functional Theory), 709; B. S. Juršić, *Tetrahedron,* 1997, **53**, 13285; B. S. Juršić, *J. Chem. Soc., Perkin. Trans. 2,* 1996, 1021.
20. C. Olea-Azar and J. Parra-Mouchet, *J. Mol. Struct. (Theochem),* 1997, **390**, 239.
21. A. V. Arbuznikov, L. A. Sheludyakov, and E. B. Burgina, *Chem. Phys. Lett.,* 1995, **240**, 239.
22. A. M. Sapse, G. Snyder, and A. V. Santoro, *J. Phys. Chem.,* 1981, **85**, 662.
23. W. G: Herkstroeter, *J. Am. Chem. Soc.,* 1973, **95**, 8686.
24. W. Kinasiewicz, A. Leš, and I. Wawer, *J. Mol. Struct. (Theochem),* 1988, **168**, 1.
25. J. B. Lambert and Y. Takeuchi, (eds.), 'Acyclic Organonitrogen Stereodynamics', VCH, 1991, p. 224.

26. A. M. Sapse, G. Snyder, and A. V. Santoro, *J. Phys. Chem.,* 1981, **85**, 662; G. L. Kenyon, G. E. Struve, P. A. Kollman, and T. I. Moder, *J. Am. Chem. Soc.,* 1976, **98**, 3695.
27. P. V. Bharatam and P. Iqbal, *J. Comp. Chem.,* 2006, **27**, 334.
28. S. Herres-Pawlis, A. Neuba, O. Seewald, T. Seshadri, H. Egold, U. Floerke, and G. Henkel, *Eur. J. Org. Chem.,* 2005, 4879.
29. **Cu** S. Herres-Pawlis, U. Flörke, and G. Henkel, *Acta. Cryst.,* 2005, **E61**, m79; S. H. Oakley, M. P. Coles, and P. B. Hitchcock, *Inorg. Chem.,* 2003, **42**, 3154. **Fe** S. Pohl, M. Harmjanz, J. Schneider, W. Saak, and G. Henkel, *J. Chem. Soc., Dalton. Trans.,* 2000, **19**, 3473. **Fe Zn** H. Wittmann, V. Raab, A. Schorm, J. Plackmeyer, and J. Sundermeyer, *Eur. J. Inorg. Chem.,* 2001, **8**, 1937. **Zn** U. Köhn, M. Schulz, H. Görls, and E. Anders, *Tetrahedron Asymm.,* 2005, **16**, 2125; H. Wittmann, A. Schorm, and J. Sundermeyer, *Z. Anorg. Allg. Chem.,* 2000, **626**, 1583. **Cd** I. M. Muller and R. Robson, *Angew. Chem. Int. Ed.,* 2000, **39**, 4357. **Co** P. J. Bailey, K. J. Grant, S. Pace, S. Parsons, and L. J. Stewart, *J. Chem. Soc., Dalton Trans.,* 1997, **22**, 4263.
30. S. Herres, U. Flörke, and G: Henkel, *Acta Cryst.,* 2004, **C60**, m659.
31. M. Fotsing Kamte, C. Wagner, and W. Schäfer, *Anal. Sci.,* 2005, **21**, 5; K. Jong Lee, I. Yoon, S. Sung Lee, and B. Yong Lee, *Bull. Korean Chem. Soc.,* 2002, **23**, 399.
32. L. He, L. Chunhe, and Z. Bohua, *Chem. J. on Internet,* 2004, **6**, 44.
33. R. Kakkar, R. Grover, and P. Gahlot, *J. Mol. Struct. Theochem.,* 2006, **767**, 175.
34. D. V. Deubel and L. Kai-Chi, *Chem. Commun.,* 2006, 2451.
35. The Irving-Williams order of stability constants for the divalent metal ions is: Pd(II) > Cu(II) > Ni(II) > Co(II) > Zn(II) > Mn(II), H. Sigel and D. B. McCormick, *Acc. Chem. Res.,* 1970, **3**, 201; R. B. Martin, *J. Chem. Educ.,* 1987, **64**, 402.
36. Gaussian 03, Revision B.03, M. J. Frisch, G. W. Trucks, H. B. Schlegel, G. E. Scuseria, M. A. Robb, J. R. Cheeseman, J. A. Montgomery, Jr., T. Vreven, K. N. Kudin, J. C. Burant, J. M. Millam, S. S. Iyengar, J. Tomasi, V. Barone, B. Mennucci, M. Cossi, G. Scalmani, N. Rega, G. A. Petersson, H. Nakatsuji, M. Hada, M. Ehara, K. Toyota, R. Fukuda, J. Hasegawa, M. Ishida, T. Nakajima, Y. Honda, O. Kitao, H. Nakai, M. Klene, X. Li, J. E. Knox, H. P. Hratchian, J. B. Cross, C. Adamo, J. Jaramillo, R. Gomperts, R. E. Stratmann, O. Yazyev, A J. Austin, R. Cammi, C. Pomelli, J. W. Ochterski, P. Y. Ayala, K. Morokuma, G. A. Voth, P. Salvador, J. J. Dannenberg, V. G. Zakrzewski, A. Dapprich, A. D. Daniels, M. C. Strain, O. Farkas, D. K. Malick, A. D. Rabuck, K. Raghavachari, J. B. Foresman, J. V. Ortiz, Q. Cui, A. G. Gaboul, A. Clifford, J. Cioslowski, B. B. Stefanov, G. Liu, A. Liashenko, P. Piskorz, I. Komaromi, R. L. Martin, D. J. Fox, T. Keith, M. A. Al-Laham, C. I. Peng, A. Nanayakkara, M. Challacombe, P. M. W. Gill, B. Johnson, W. Chen, M. W. Wong, C. Gonzalez, and J. A. Pople, *Gaussian, Inc.,* Pittsburgh PA, 2003.
37. J. M. Seminario and P. Politzer, (eds.), 'Modern Density Functional Theory: A Tool for Chemistry', Theoretical and Computational Chemistry 2, Elsevier, Amsterdam, 1995.
38. A. D. Becke, *J. Chem. Phys.,* 1993, **98**, 1372.
39. C. Lee, W. Yang, and R. G. Parr, *Phys. Rev. B,* 1988, **37**, 785.

40. S. Miertus, E. Scrocco, and J. Tomasi, *J. Chem. Phys.,* 1981, **55**, 117; B. Mennucci and J. Tomasi, *J. Chem. Phys.,* 1997, **106**, 5151.
41. B. Kovačević and Z. B. Maksić, *Org. Lett.,* 2001, **3**, 1523.